Available online at www.sciencedirect.com
ScienceDirect
Catalysis Today 129 (2007) 96–101
CATALYSIS TODAY
www.elsevier.com/locate/cattod

Photocatalytic degradation of volatile organics on TiO_2 embedded glass spherules

D.S. Tsoukleris [a], T. Maggos [b], C. Vassilakos [b], P. Falaras [a,*]

[a] *Institute of Physical Chemistry, NCSR "Demokritos", 153 10 Aghia Paraskevi Attikis, Greece*
[b] *Environmental Research Lab/INT-RP, NCSR "Demokritos", 153 10 Aghia Paraskevi Attikis, Greece*

Available online 7 August 2007

Abstract

This work investigates the feasibility of applying photocatalytic technology for removal of volatile organic compounds (VOCs) over TiO_2. A photocatalytic packed bed reactor (PPBR) was employed to determine the oxidation rates of VOCs (bezene, toluene, *o*-, *m*-, *p*- xylenes). TiO_2 Degussa P25 was used to prepare a nanocrystalline titania paste, where glass spherules were embedded. The photocatalyst was extensively characterized by means of spectroscopy (Raman, XRD) and microscopy (SEM, AFM). Experiments were conducted under 'real world setting' condition of temperature (25 °C ±2) and humidity (60%) while the irradiation was provided by 15 W near UV lamps. The dependence of the reaction rate on light intensity as well as the deactivation of the catalyst were determined. The results indicate that the rate of the photo-oxidation process increased while increasing the intensity of UV irradiation. Using two (2) UV-A lamps, the destruction rate of benzene and toluene was 0.0429 and 0.1960 $\mu g\, m^{-2}\, h^{-1}$ respectively, while with four (4) UV-A lamps values of 0.6775 and 1.5301 $\mu g\, m^{-2}\, h^{-1}$ correspondingly were obtained. The stabilized photocatalysts present remarkable stability (no deactivation and excellent repeatability). Reproducibility tests proved that the photocatalytic activity of the photocatalyst remains intact even after thirty consecutive experiments of new added VOCs quantities.

Keywords: VOCs; Photocatalytic degradation; Photocatalysis; PPBR; Titanium dioxide

1. Introduction

Most volatile organic compounds (VOCs) are known as carcinogens (i.e., benzene), while some others (toluene, xylenes) are associated with acute effects [1–7]. Therefore, there is a great demand to develop environmental friendly and cost effective methods for their destruction. Heterogeneous photocatalysis is an advanced oxidation process (AOP), very useful for the treatment of air polluted with VOCs. The method has received a major interest during the last years and become a very promising technique for the remediation of environmental pollution, because it can totally destruct organic molecules at a low energy cost. Titanium dioxide (TiO_2) photocatalytic reactions have an advantage over other reactions, such as thermal and catalytic incineration in that they can efficiently decompose low concentrations of VOCs under mild conditions [8–10]. Although, there is a lot of published research in the area of photocatalysis, there is a lack of information regarding photocatalytic reactor configuration together with photocatalyst nature and substrate. Recently, we reported on the design, fabrication and theoretical modelling of a new gas-phase photocatalytic packed bed reactor PPBR (Fig. 1), conceived for incorporating titania photocatalysts for VOCs destruction [11]. To complete the work and confirm the applicability of the above system, the investigation of the decomposition kinetics of organic compounds over TiO_2 at the PPBR is necessary. For efficiency optimization reasons, the main component to be controlled and adapted to the PPBR is the photocatalytic material. For this reason, we developed a paste based on commercial titanium dioxide powder that leads to porous nanostructured titania materials and we used small glass spherules as the substrate and have a more efficient contact between the semiconductor and the pollutants. Our photocatalyst is immobilized onto the surface of the glass spherules which are used to fill-in the pyrex glass tube of the PPBR. Thus, the current work evaluates the technical viability of the titanium dioxide (TiO_2) photocatalysts to the removal of the main VOCs present in ambient air, at parts per billion (ppb) concentrations [12].

* Corresponding author. Tel.: +30 210 6503644; fax: +30 210 6511766.
E-mail address: papi@chem.demokritos.gr (P. Falaras).

0920-5861/$ – see front matter
doi:10.1016/j.cattod.2007.06.047

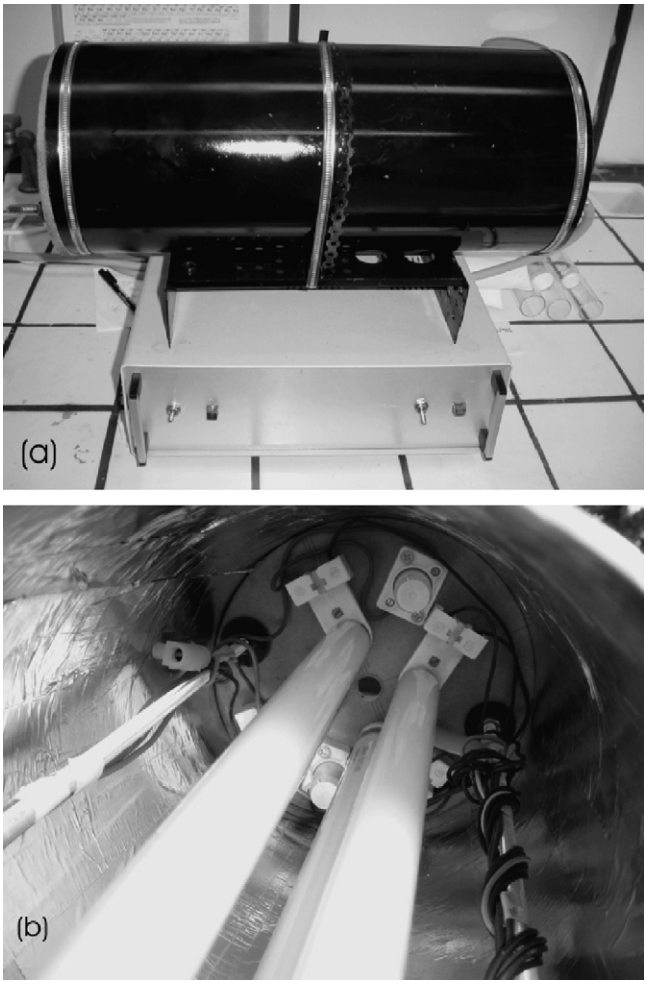

Fig. 1. The photocatalytic packed bed reactor (PPBR) used in this study: (a) outer and (b) inner views. Operation is possible with four or two lamps.

2. Experimental

2.1. Preparation of TiO_2 paste

Synthetic methods aiming at preparing efficient pastes of titanium dioxide are of great interest. The composition of the precursor paste is crucial for the homogeneity, adherence and roughness of the final TiO_2 porous films. In this work, commercially available TiO_2 powder (Degussa P25) was thoroughly used for the preparation of the titania pastes, due to its nanoparticle characteristics and availability. Essential parameters, such as paste components, addition of binder molecules and dispersion temperature are examined. Prior to paste preparation, the semiconductor powder was heated overnight at 200 °C in order to remove excess moisture. The exact composition of the paste is shown in Table 1.

The surface modifier is a 10% aqueous solution of acetyl-acetone. Primarily, 0.5 g of TiO_2 were mixed with 2.3 ml of the acetyl-acetone surface modifier solution to produce a mixture [13]. The addition of the semiconductor powder and water (1.5 ml) is slow and the mixture is homogenized under continuous stirring for 60 min. Then, three drops of the binder (Triton X-100) were added. Mechanical stirring of the final paste continues for at least 2 h. At the end, the paste is treated in an ultrasonic bath for 1 h, in order to assure the total absence of titanium dioxide aggregates.

Table 1
Concentration of VOCs as a function of the illumination time (four UV-lamps)

	Benzene ($\mu g/m^3$)	Toluene ($\mu g/m^3$)	*m*, *p*-Xylene ($\mu g/m^3$)	*o*-Xylene ($\mu g/m^3$)
Blank (inactive UV-lamps)	775.2	1321.7	74.1	45.4
1 min UV	304.7	259.1	–	–
2 min UV	112.4	31.5	–	–
3 min UV	110.8	0.0	–	–

2.2. Paste deposition and treatment

The produced paste was deposited into the surface of small glass spherules of 0.5 cm in diameter. All the spherules were ultrasonically cleaned in ethanol prior to use and put into the paste for 5 min under vigorous stirring. The glass spherules supported with a thin layer of titania paste were dried at 120 °C for 15 min and annealed at 450 °C for exactly 90 min. This thermal treatment assured the removal of the organic load and facilitated interconnection (sintering) of titanium dioxide nanoparticles.

2.3. Characterization of TiO_2 photocatalysts

The crystallinity of the titanium dioxide photocatalysts was studied with a Siemens D-500 X-ray diffractometer, using Cu Kα radiation. Raman spectroscopy was employed to elucidate the vibrational modes of the semiconductor. Raman measurements were carried out with a triple Jobin–Yvon spectrometer equipped with a microscope and a CCD detector and a 514.5 nm Argon laser. Detailed surface images were obtained by means of a scanning electron microscope (SEM) with numerical image acquisition (LEICA S440). Carbon deposition has been performed to avoid problems arising from surface charge effects. X-ray from the SEM microscope probe (at horizontal incidence beam) was used for non-destructive qualitative and quantitative chemical analysis of the modified films. Surface morphology, roughness and fractality of the titania photocatalysts were examined with a digital instruments nanoscope III atomic force microscope (AFM), operating in the tapping mode (TM) [12,13].

2.4. Photocatalytic experiments

The photocatalytic activity of the PPBR with TiO_2 was evaluated by the photo-degradation of benzene, toluene and *o*-, *m*-, *p*-, xylenes (BTX). The pollutant molecular weights are 78, 92 and 106, respectively.

Photocatalysis experiments were carried out at the PPBR. The small glass spherules covered with titania photocatalyst were put inside the pyrex (permitting radiation pass when wavelength is over 320 nm) glass tube (50 cm in length and 1 cm in diameter), which in turn was incorporated in the central

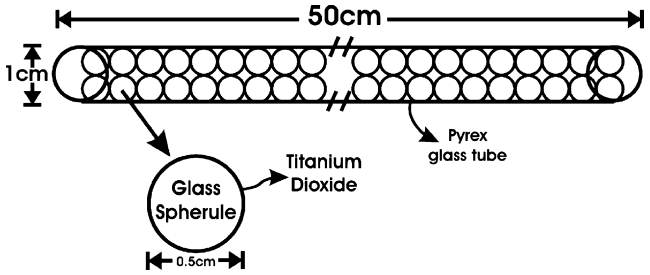

Fig. 2. Schematic diagram of pyrex glass tube and glass spherules with the photocatalyst.

axis of the photoreactor (Fig. 2). The test procedure lies first in the determination of VOCs (mixture of benzene, toluene, *o*-, *m*-, *p*-xylenes) concentration without irradiation (dark) as reference and then the measurement of VOC concentration in irradiated condition. The analytical method for BTX determination is based on adsorption on a solid substrate (Tenax-TA), followed by a Thermal-desorption unit (Chrompack) coupled to a GC-FID (HP 5890) analysis. Taking into account the airflow and the sample area, the photocatalytic destruction rate of the employed system in the given conditions, variable parameters such as pollutant flow, concentration and irradiation exposure time, can be examined and optimized [11].

As irradiation source Sylvania F15W T8/BLBlue lamps were used, each one having maximum emission of 71.5 μW cm^{-2} at 350 nm, at a distance of 25 cm. The lamps were placed in symmetrical way around the centered glass tube. Both the axis of each lamp and the pyrex glass tube were parallel. The side distance of the lamp from the glass tube was 5 cm while the same distance from the metal wall was 1.5 cm. To examine the role of the UV-intensity on the degradation efficiency, two different experiments were considered. At the first experiment illumination through four lamps was provided, while at the second one, only two (out of four) lamps were used.

3. Results and discussion

3.1. Surface properties

The total TiO_2 surface area developed on the glass spherules is about 50 cm^2. The obtained titania films are opaque and extremely rough. Their thickness was determined by an Ambios Technology (XP-2) profilometer and found to be about 20 μm.

X-ray diffraction results of the titania films after sintering at 450 °C, shown in Fig. 3, indicate a well organized crystal structure of titania nanoparticles. The inset picture zooms at the A(1 0 1) anatase and R(1 1 0) rutile peaks in the region of 24–28° [14]. The ratio of the two peak intensities was approximately the same (under the experimental error), for the new photocatalyst and Degussa P25 powder, indicating similar weight percentages of the anatase to rutile phases. The rutile content in the film is roughly 25%, while the anatase content is about 75%. This confirms that the initial crystalline composition remains in the modified catalysts. Furthermore, the grain size (*D*) was determined from the width at half maximum (*w*) of the A(1 0 1) anatase peak according to the Scherrer formula [8].

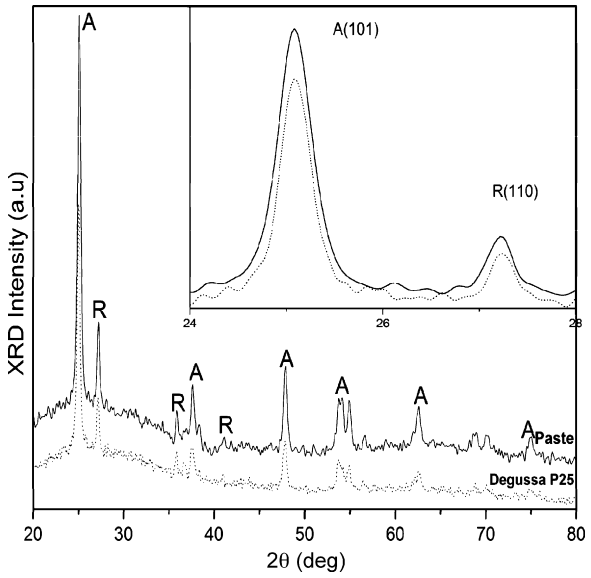

Fig. 3. The XRD patterns of titania photocatalyst.

A value of $D = 20 \pm 1$ nm was estimated for the catalysts (to compare with a value of $D = 24 \pm 1$ nm, estimated for Degussa P25).

Raman spectroscopy was used to elucidate the structural modification of the TiO_2 nanocrystalline films. The Raman spectra, Fig. 4, shows that the materials are well crystallized, without overlapped peaks and low number of imperfect sites. The anatase and rutile phases are easily distinguishable as peaks from each crystalline phase are clearly separated in frequency. Vibration peaks at 142 ± 2 cm^{-1} (E_g, vs), 194 ± 3 cm^{-1} (E_g, w), 393 ± 2 cm^{-1} (B_{1g}, s), 512 ± 1 cm^{-1} (A_{1g}, s), 634 ± 2 cm^{-1} (E_g, s) are unambiguously attributed to the anatase modification [15–18]. Although, anatase nanoparticles are the predominant species, rutile phase is also observed as a broad peak at 446 cm^{-1}. Moreover, the investigation technique confirmed the high quality of thermal annealing, as vibrations from carbonic species were not detected.

Surface morphology is the most crucial factor for an efficient thin film photocalyst. Analysis performed by means of scanning

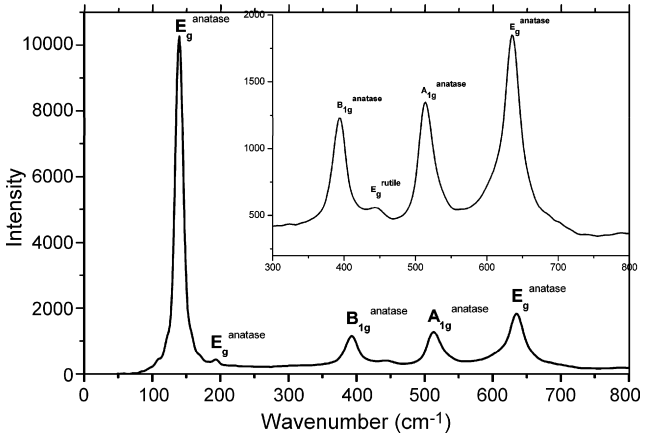

Fig. 4. Raman spectra of TiO_2 photocatalyst.

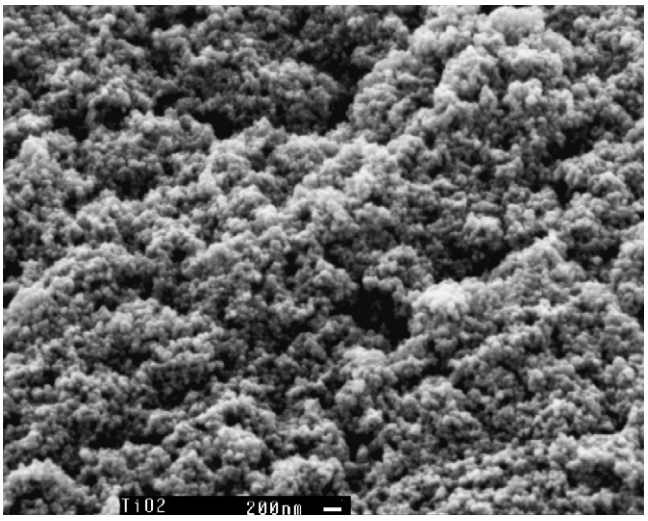

Fig. 5. Microscopic characterization of the titania films (SEM).

electron microscopy (SEM) (Fig. 5) revealed that the surface of the titania films possess a sponge like structure, with extended roughness and complex characteristics. The mean diameter of the nanocrystallites is controlled by the original semiconductor material, namely Degussa P25. Modification with an organic carrier does not induce aggregation or additional growth of the TiO_2 nanoparticles. In general, the appearance of the films resembles to a porous network with extended surface area, ideal for heterogeneous energy conversion processes, such as the photocatalytic procedure.

In order to better understand the titanium dioxide features and express this in terms of surface parameters, we have undertaken their characterization by atomic force microscopy. Fig. 6a and b presents top view and surface plot images (two- and three dimensional representations, respectively) for the modified film photocatalysts. The films consist of interconnected grain particles fused together to form the semiconductor solid material. The average grain diameter of the samples is about 20 nm, in excellent agreement with the X-ray diffraction results. The particles built up high mountains and deep valleys and their height histogram shows a Gaussian-like distribution with a maximum 145 nm for our films. Our paste produces films with surface characteristics of lower size. These results are in accordance with the roughness analysis. The r_{ms} (r_{ms} = the standard deviation of the Z values, Z being the total height range analysed) values show that our films exhibit elevated values of roughness (r_{ms}): 21.24 nm.

Looking carefully at the top-view image (two-dimensional picture) one can see that the films printed from our paste show a complex configuration. In order to evaluate and compare the geometric complexity of the film surfaces, qualitative analysis including measurements of parameters such as feature frequency and fractal dimension D_f [19] (a parameter which reflects the scaling behaviour and is an intrinsic property of the material, $3 \geq D_f \geq 2$) was performed. The fractal analysis provided a D_f value of 2.09 (± 0.02) and proved that the prepared films exhibit a relatively poor self-affine scaling character. The fractal dimension (D_f) parameter influences the

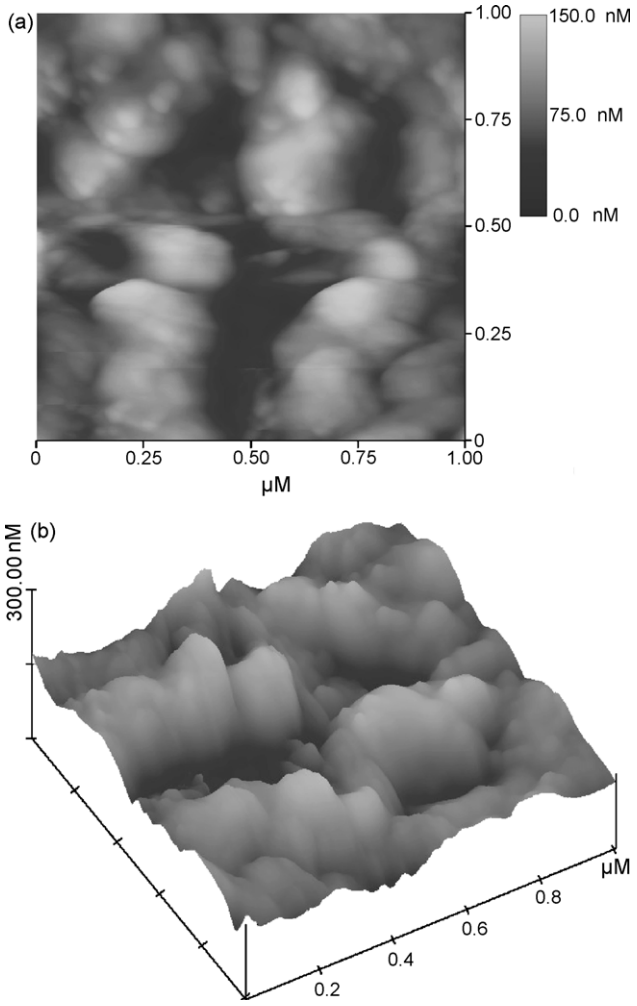

Fig. 6. AFM characterization of the titania films: (a) AFM top view (two dimensional image); (b) surface plot (3-D image).

effective surface extension and therefore fractal films show a higher ability to efficiently capture photons, through a complex semiconducting network acting in a ''sponge''-like way. The grain diameter of the TiO_2 nanoparticles is also an essential parameter [20]. Finally, taking into account the heterogeneous photocatalytic mechanism of a thin film TiO_2 catalyst [21], the height and roughness of surface features must be considered. The films have a complex surface structure and present increased roughness resulting from surface characteristics of important height. As a result, these films are endowed with a high real surface extension, which readily favours the photodecomposition process. In fact, such a surface not only permits the adsorption of a greater number of pollutant molecules, but also creates a rough environment where multiple light reflections can occur, thus considerably increasing the amount of the adsorbed photons.

3.2. Photocatalytic efficiency

The photoreactor allows varying flow rate, gas composition, humidity, and temperature. The experimental setup permits us to follow the behaviour of VOCs under UV illumination. The

determination of the photocatalytic activity proceeds as follows. Under dark conditions (all UV-lamps were inactive), a purified air flow of 110 ml min^{-1} is established in order to allow possible pollutants to be desorbed from the specimen. A sample is taken after 2 h to check the cleanness of the system. Then the reactor is connected to a gas cylinder containing a known concentration of BTX with specific air flow rate (110 ml min^{-1}) passed inside the glass tube. The system is allowed to equilibrate for at least 3 h and a series of three samples is taken (1 h sampling interval). The amount of each pollutant measured at this stage give the non-irradiated (dark) steady-state concentration. The UV irradiation is then activated and a significant elimination of the pollutants concentration was observed. While waiting for the system to equilibrate, the concentration of the pollutants turned almost to zero. Consequently, samples were taken only after few minutes from the activation of the UV source. After that UV irradiation is turned off and the system is allowed to re-equilibrate in order to confirm previously measured BTX ''dark'' concentration levels.

The obtained results, listed in Table 1, shows that the concentration of VOCs (starting at 775.2, 1321.7, 74.1 and 45.4 $\mu g/m^3$ for benzene, toluene, *m*-, *p*- and *o*-xylene, respectively) is a function of the illumination time. After 3 min the concentration goes down to 110.8 $\mu g/m^3$ for benzene. All the mass of toluene has been practically destroyed after 3 min. Data for *o*-, *m*-, *p*-xylenes are not given, as these pollutants completely disappear even at 1 min of illumination.

The photocatalytic rate of VOC destruction in mass per unit of area per unit of time ($\mu g\ m^{-2}\ h^{-1}$) was determined by using the eq. (1):

$$\text{DestrRate} = \frac{(C_{\text{dark}} - C_{\text{irrad}})\text{GasFlow}}{\text{SampArea}} \quad (1)$$

where DestrRate is the rate of VOC destruction in mass per unit area and per unit time ($\mu g\ m^{-2}\ h^{-1}$), C_{dark} the VOC concentration in the steady-state dark phase of the experiment ($\mu g\ m^{-3}$), C_{irrad} the VOC concentration in the steady-state irradiation phase of the experiment ($\mu g\ m^{-3}$), GasFlow the air volume variation in the experimental chamber ($m^3\ h^{-1}$) and SampArea is the area of the photocatalyst (m^2). Using equation (1), the photodegradation rates for the different aromatic compounds were obtained, concerning illumination via 4 UV-A lamps. The results show that the destruction rate of benzene and toluene at the first minute is 0.173 and 0.390 $\mu g\ m^{-2}\ s^{-1}$, at the second minute 0.071 and 0.083 $\mu g\ m^{-2}\ s^{-1}$ and at the third minute 0.001 and 0.012 $\mu g\ m^{-2}\ s^{-1}$, respectively. In addition, the destruction rates of *m*,*p*-xylene and *o*-xylene at the first minute were 0.03 and 0.02 $\mu g\ m^{-2}\ s^{-1}$, correspondingly.

Assuming a linear correlation between pollutant average concentration, C_{av} ($\mu g\ m^{-3}$) (in the gas phase during photocatalysis) and destruction rate, DestrRate, it is possible to describe the catalytic activity with a linear fitting of the data. Particularly, considering an original constrained linear fitting, the catalytic activity, CatAct [in $m\ h^{-1} = (\mu g\ m^{-2}\ h^{-1})/(\mu g\ m^{-3})$], of every sample–substrate pair is expressed with a single parameter that does not depend on the pollutant concentration:

$$\text{CatAct} = \frac{\text{DestrRate}}{C_{\text{av}}} \quad (2)$$

The application of equation (2) gives the catalytic activity of VOC destruction for benzene and toluene with 4 UV-A lamps: this is 320×10^{-6} and 493×10^{-6} m $s^{-1}$for the first minute, 338×10^{-6} and 574×10^{-6} m s^{-1} for the second minute and 5×10^{-6} and 733×10^{-6} m s^{-1} for the third minute, respectively. The corresponding value (for the first minute) for the *m*,*p*, and *o*-xulenes was 733×10^{-6} m s^{-1}.

Table 2
Concentration of VOCs as a function of the illumination time (two UV-lamps)

	Benzene ($\mu g/m^3$)	Toluene ($\mu g/m^3$)	*m*, *p*-Xylene ($\mu g/m^3$)	*o*-Xylene ($\mu g/m^3$)
Blank (inactive UV-lamps)	701.2	1170.4	–	–
1 min UV	674.8	773.0	–	–
2 min UV	518.6	175.8	–	–
3 min UV	288.7	40.15	–	–

3.3. UV intensity effect

In order to see the influence of the UV intensity on the photocatalytic efficiency, the experiments were again performed using the two lamp configuration. The results, reported on Table 2, indicate much lower photocatalytic degradation in all the gas components. The initial concentration of benzene and toluene is 701.2 and 1170.4 $\mu g/m^3$, respectively while after 3 min these concentration comes of 288.7 and 40.15 $\mu g/m^3$, respectively. The destruction rates of benzene and toluene at the first minute are 0.010 and 0.146 $\mu g\ m^{-2}\ s^{-1}$, at the second minute 0.057 and 0.219 $\mu g\ m^{-2}\ s^{-1}$ and at the third minute 0.084 and 0.050 $\mu g\ m^{-2}\ s^{-1}$, respectively. The catalytic activity of benzene and toluene at the first minute becomes 14×10^{-6} and 150×10^{-6} m s^{-1}, at the second minute 96×10^{-6} and 462×10^{-6} m s^{-1} and finally at the third minute 209×10^{-6} and 461×10^{-6} m s^{-1}, respectively. The above results clearly demonstrate that a lower efficiency is due to the significantly lower light intensity provided by the two lamps configuration.

3.4. Stability tests

The nanocrystaline titania spherules were continuously tested as photocatalysts for checking their lifetime and stability. The tests (more than 30 photocatalytic experiments conducted at a frequency of about five experiments per month) covered a 6-month period during which no sign of activity loss, decrease or time dependence was observed. The obtained results for the deactivation of the catalyst are represented on Table 3. We can see that even after 30 consecutive experiments of new added VOCs quantities at a 6-month period our photocatalyst remained active. The absence of Raman peaks in

Table 3
Stability tests (catalyst deactivation)

Experiments	CatAct (m h^{-1}) after 3 min (four UV-A lamps)	
	Benzene	Toluene
1st	2.06×10^{-5}	1.44×10^{-3}
5th	1.99×10^{-5}	1.41×10^{-3}
10th	2.01×10^{-5}	1.37×10^{-3}
15th	2.13×10^{-5}	1.40×10^{-3}
20th	1.96×10^{-5}	1.43×10^{-3}
25th	2.03×10^{-5}	1.39×10^{-3}
30th	1.95×10^{-5}	1.36×10^{-3}

the aromatic region on the used titania modified glass spherules, exclude deposition of pollutant (in the form pf carbon or pollutant intermediates) that could deactivate the photocatalyst.

4. Conclusions

The ability of the PPBR to destruct volatile organic compounds (mixture of benzene, toluene and xylenes) has been investigated using titanium dioxide photocatalysts supported on glass spherules under UV-A illumination. The PPBR has been recognized as an important vehicle that can lead to study of the destruction of many VOCs (benzene, toluene, *o*-, *m*-, *p*-xylenes). From our results we can confirm that conversion efficiencies higher than 90% can be easily achieved. This reactor can provide effortless, low-cost manufacture and increased efficiency, even at an elevated pollutant feed.

We have proven that the glass supported titania photocatalyst materials are fully compatible with the simple but judicious design of the packed bed photoreactor. The system is very versatile and direct applications, including its practical use for the photodecomposition of numerous gas pollutants, can now be considered. The obtained results make further work on the subject very encouraging. In fact, such a simple, one step and low cost method for photocatalyst preparation permits the catalyst immobilization and present the advantage of easier photocatalysts separation. In addition, the remarkable stability observed opens the possibility to develop and use more efficient photocatalysts in the form of porous and high surface area inorganic oxide matrixes (i.e., foams) by using different precursor materials.

Acknowledgements

Great acknowledgements are expressed for financial support from General Secretariat for Research and Development (GSRT/Ministry of Development, Greece) through 03EΔ118/2005 ''PENED'', 4.5/4.4.1, Competiveness/Infrastructure (''EPAN YPODOMON'') and Greek-British bilateral projects. Thanks must also be addressed to Dr. M.C. Bernard for SEM pictures and for Raman investigations.

References

[1] International Agency for Research on Cancers (IARC), Monographs on the evaluation of carcinogenic risk to humans, Supplement 7, 1987.
[2] L.A. Wallace, Cancer risk from organic chemicals in homes, in: Proceedings of Environmental Risk Management, APCA, Pittsburgh, PA, 1986, pp. 14–24.
[3] US Environmental Protection Agency (USEPA), Cancer risk from outdoor exposure to air toxics PA-450/1-90-004a, 1990.
[4] J. Peral, D.F. Ollis, J. Catal. 134 (1992) 554.
[5] T.N. Obee, R.T. Brown, Environ. Sci. Technol. 29 (1995) 1223.
[6] X. Fu, L.A. Clark, W.A. Zeltner, M.A. Anderson, J. Photochem. Photobiol. A: Chem. 97 (1996) 181.
[7] M.R. Nimlos, E.J. Wolfrum, M.L. Brewer, J.A. Fennel, G.B. Bintner, Environ. Sci. Technol. 30 (1996) 3102.
[8] X.F. Fu, W.A. Zeltner, M.A. Anderson, Appl. Catal. B Environ. 6 (1995) 209.
[9] W.A. Jacoby, D.M. Blake, J.A. Fennell, J.E. Boulter, L.M. Vargo, Air. Waste Manage. Assoc. 46 (1996) 891.
[10] J. Blanco, P. Avila, A. Bahamonde, E. Alvarez, B. Sanchez, M. Romero, Catal. Today 29 (1996) 437.
[11] I.M. Arabatzis, N. Spyrellis, Z. Loizos, P. Falaras, J. Mater. Proces. Techn. 161 (2005) 224.
[12] Julian Blanco Galvez, Sixto Malato Rodríguez, Solar Detoxification, United Nations Educational, 2003, p.2.
[13] D.S. Tsoukleris, I.M. Arabatzis, E. Chatzivasiloglou, A.I. Kontos, V. Belessi, M.C. Bernard, P. Falaras, J. Solar Energy 9 (2005) 422.
[14] JCPDS Powder Diffraction File, Card 21-1272, JCPDS, International Centre for Diffraction Data, Swarthmore, PA, (1980).
[15] H.P. Klug, L.E. Alexander, X-ray Diffraction Procedures, Wiley, New York, 1954 (Chap. 9).
[16] V.V. Yakovlev, G. Scarel, C.R. Aita, S. Mochizuki, Appl. Phys. Lett. 76 (2000) 1107.
[17] A. Turkovic, M. Ivanda, A. Drasner, V. Vranesa, M. Persin, Thin Solid Films 198 (1991) 199.
[18] P. Falaras, A. Hugot-Le Goff, M.C. Bernard, A. Xagas, Sol. Energy Mater Sol. C. 64 (2000) 167.
[19] A. Provata, P. Falaras, A. Xagas, Chem. Phys. Lett. 297 (1998) 484.
[20] N. Serpone, D. Lawless, R. Khairutdinov, E. Pelizzetti, J. Phys. Chem. 99 (1995) 16655.
[21] N. Serpone, A. Salinaro, A. Emeline, V. Ryabchuk, J. Photochem. Photobiol. A 130 (2000) 83.